

# Assessment of Murine Neuroblastoma (N1E-115) Resting Membrane Potential by Confocal Microscopy

Miguel Hernandez,<sup>1</sup> William S. Kisaalita,<sup>1,3</sup> and Mark A. Farmer<sup>2</sup>

Received July 25, 1995; accepted April 23, 1996

Digital imaging (confocal microscopy) and a slow potentiometric dye (tetramethylrhodamine methyl ester) were used to assess the resting membrane potential ( $V_m$ ) of murine neuroblastoma cells (N1E-115). The average  $V_m$  was found to be  $-64.0 \pm 2.0$  mV. The difference between this and the previously reported higher values was attributed to the use of glass microelectrode techniques that probably caused mechanical injury to the cell membranes. Digital imaging of N1E-115  $V_m$  was found to be sensitive, reproducible, fast, and simple.

**KEY WORDS:** Resting membrane potential; tetramethylrhodamine methyl ester; confocal microscopy; neuroblastoma; N1E-115.

## INTRODUCTION

We have an interest in using neuroblastoma cells as an *in vitro* model for neurotoxicity testing, with alteration in resting membrane potential ( $V_m$ ) as the end point.<sup>(1)</sup> For most cell lines of nervous system origin, low transmembrane potential characterize exponentially growing cells and the transition from log to stationary growth phase is marked by a shift toward large transmembrane potential values. A further hyperpolarization occurs when the cells undergo differentiation. Differentiated cells characteristically have more homogeneous  $V_m$  values ranging from  $-45$  to  $-90$  mV.<sup>(2,3)</sup> However,  $V_m$  interpretation based on microelectrode intracellular recording and whole-cell patch-clamp measurements remains a matter of dispute.<sup>(4)</sup> One point of view is that the observed values are real and that  $V_m$  is a developmentally regulated property. The other view is that low

$V_m$  transmembrane potential values are experimental artifacts that reflect uncertainties associated with glass microelectrode techniques, which include the possibility of mechanical injury to the membrane with intracellular recording and the need to match the pipet electrolyte and the cytosol ionic compositions in the whole-cell clamp configuration.<sup>(5,6)</sup> For these reasons, the use of voltage-dependent fluorescent dyes is gaining popularity, because the uncertainties associated with dye accumulation are quite different. Numerous potentiometric dye applications have been reviewed by Loew.<sup>(7,8)</sup> In this note we report the use of a slow potentiometric dye (tetramethylrhodamine methyl ester; TMRM) and digital imaging (confocal microscopy in the photon counting mode) to quantitatively measure murine neuroblastoma (N1E-115) resting membrane potential.

## MATERIALS AND METHODS

### Potentiometric Dye

Tetramethylrhodamine methyl ester (TMRM; Molecular Probes) was chosen in this study for several rea-

<sup>1</sup> Biological and Agricultural Engineering Department, Driftmier Engineering Center, University of Georgia, Athens, Georgia 30602-4435.

<sup>2</sup> Department of Cellular Biology, Center for Advanced Ultrastructural Research, University of Georgia, Athens, Georgia 30602-4435.

<sup>3</sup> To whom correspondence should be addressed.

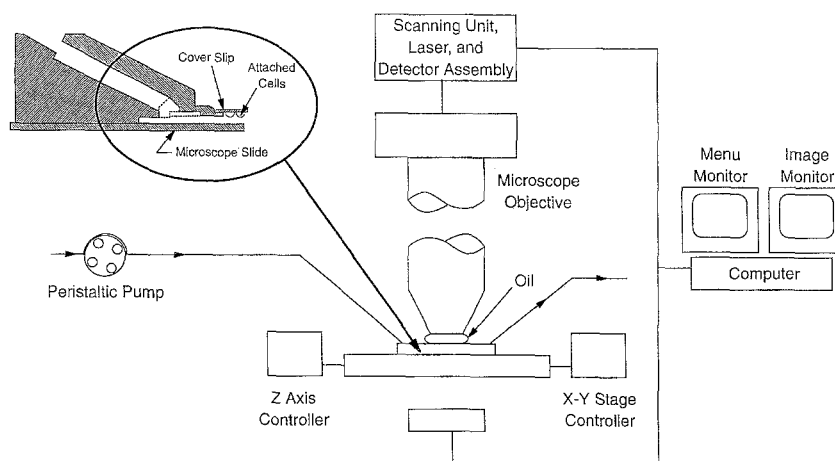


Fig. 1. Schematic of the confocal microscopy experimental setup.

sons: TMRM (1) exhibits low non-specific binding and therefore readily displays reversible potential dependent uptake, (2) is not quenched when taken up by mitochondria and therefore cytoplasmic and mitochondrial fluorescence are readily distinguished, and (3) is non-toxic to most cells.<sup>(6,9)</sup>

### Cell Culture

N1E-115 cells of passage 12 were obtained from Dr. M. Nirenberg of the National Institute of Health. A previously published protocol<sup>(10)</sup> was followed. Briefly, N1E-115 cells were grown to confluence in 75-cm<sup>2</sup> culture flasks (Costar) in Dulbecco's modified Eagle's minimal essential medium (DMEM) containing 0.12% NaHCO<sub>3</sub> and supplemented with 13% fetal bovine serum (FBS), 2% L-glutamine, 120 U/ml penicillin, and 12 U/ml streptomycin. The cultures were maintained at 37°C in a humidified atmosphere containing 10% CO<sub>2</sub>.

### Confocal Microscopy

A schematic of the experimental setup is shown in Fig. 1. The flow chamber used is similar to that previously described by Berg and Block.<sup>(11)</sup> A peristaltic pump was used to allow rapid flow of medium through the longitudinal chamber channel along its entire width. Temperature control of the samples during microscopic observation was achieved with an air stream stage incubator (ASI 400, Nicholson Precision Instruments). Unless otherwise stated, all experiments were carried out at 18°C. A confocal imaging system (MRC-600, Bio-Rad Laboratories), equipped with fast photon counting elec-

tronics was used. As shown in Fig. 1, the imaging system was linked to an upright Nikon Optiphot microscope, equipped with a 60 × Apochromat, oil-immersion, high-numerical aperture (1.40) objective lens. The imaging system's krypton/argon mixed gas laser was used to excite the fluorescent dye at 568 nm, and emission scans were recorded as relative fluorescence intensities at 610 nm.

Three to five days prior to their use, N1E-115 cells were mechanically removed from the culture flasks, counted, and replated in six-well clusters (Costar), holding one 12-mm round glass coverslip, at a density of  $120 \times 10^3$  cells/well. Cultures were incubated overnight in growth medium, and the next day the growth medium was exchanged with low-serum medium (2.5% FBS), to minimize cell proliferation without inducing morphological differentiation. After 48 h under low-serum medium, the incubation was terminated by removal of the medium, followed by washing of the cells on the coverslips with Earle's balanced salt solution (EBSS). After wiping their edges and reverse sides dry, the coverslips were placed with the cells facing the interior of the flow chamber. The flow chamber was filled either with EBSS and 0.5 μM TMRM for  $V_m$  measurement or with high-potassium NaCl-free EBSS (made up of 170 mM KCl, 13.1 mM NaHCO<sub>3</sub>, 0.5 μM TMRM, and 0.1 μM valinomycin) for cell depolarization experiments. Coverslips were held in position by means of a thin film of high-vacuum silicon grease applied to the top seat of the flow chamber. Complete equilibration was taken as the time at which fluorescence measured from the cell had attained a steady intensity. Upon complete equilibration of intracellular dye distribution, the flow chamber was

placed under the Nikon Optiphot upright microscope stage and the MRC-600 system was set up for fast photon counting. The krypton/argon mixed gas laser was turned on and an appropriate focal plane of a single cell, loaded with fluorescent probe, was focused on. The sample fluorescence was recorded and the image was digitized with  $512 \times 512$ -pixel spatial and 8-bit intensity resolution via a frame grabber and stored directly to a Panasonic optical disk (940 MB). A total of 40 cells was analyzed from two independent coverslips.

Data analysis was performed with Bio-Rad COMOS image analysis software package. A rectangular area of interest (AOI) of approximately  $60 \mu\text{m}^2$  was defined via the image processor's cursor controls. This AOI was placed inside the cell in a region devoid of mitochondria and fluorescence intensity histograms were generated. The same-size AOI was then placed outside the cell, in a region devoid of processes or any other glowing debris, and the fluorescence intensity histograms were generated in a similar manner. The ratio of the mean values of the fluorescent intensities measured from inside and outside the cell ( $F_i/F_o$ ) was related to  $V_m$  by the Nernst equation:

$$V_m = -2.3 (RT/ZF) \log_{10} (F_i/F_o)$$

where  $V_m$  is the resting membrane potential in mV,  $Z$  is the charge on the TMRM ion,  $F$  is Faraday's constant,  $R$  is the ideal gas constant, and  $T$  is the absolute temperature. Fluorescence contributions from no-dye cell preparations were negligibly small ( $<0.1\%$ ) and therefore there was no need to correct  $F_i$  and  $F_o$  for background. Considering that the stage temperature was maintained at  $18^\circ\text{C}$  and assuming a  $Z$  of 1 for TMRM ion, the constant  $2.3 (RT/ZF)$  was found to be equal to 58 mV.

## RESULTS AND DISCUSSION

False-color was used to demonstrate fluorescence relative to pixel intensities, with black and red representing 0 and 250, respectively. Complete dye equilibration was achieved in approximately 5 min. As shown in Fig. 2, TMRM stained the N1E-115 cell cytosol as well as intracellular organelles. The nuclear region was stained to a lesser extent, reflecting the absence of membranous organelles, therefore the measurement of fluorescence intensity inside the cells was made at these relatively darker, uniformly stained regions. Figure 3 shows a series of typical optical sections obtained via

systematic focusing through the entire thickness of a N1E-115 cell at a  $1\text{-}\mu\text{m}$  vertical spacing. Fluorescence intensity histograms were produced for each section. The section with minimal intensity variability was selected as the optimum section for scoring intracellular fluorescence. For most cells, sections with minimal fluorescence intensity variability were found at approximately  $9 \mu\text{m}$  from the coverslip. Figure 4 shows an AOI, placed on the nuclear area and an area outside of the cell devoid of glowing debris, respectively.  $V_m$  was calculated from the ratio of the average fluorescence intensities from these two AOIs as outlined previously.

The addition of valinomycin decreased the intracellular fluorescence intensity rapidly. Under these conditions (i.e., high external  $\text{K}^+$  with valinomycin), there was no significant difference between intra- and extracellular fluorescence intensities (Fig. 5), confirming that nonspecific binding by TMRM was negligible.  $V_m$  measurements from individual cells are presented in Fig. 6. The filled squares represent the single-cell average and error bars represent  $\pm$  five times the standard error of the mean. The fact that standard deviations were less than 5% of the mean reflected excellent precision. Also, the mean value of  $-64.0$  with a 95% confidence interval of  $\pm 2.0$  mV from 40 cells indicated an excellent cell-to-cell variability, which has not been reported from cultured cells. However, the mean  $V_m$  of  $-64.0$  mV was much lower than the previously published values of  $-25$  to  $-39.8$  mV, obtained with microelectrode techniques from N1E-115 cells cultured under similar conditions.<sup>(10,12-14)</sup> Although it has been conclusively determined that  $V_m$  is a developmentally regulated property in N1E-115,<sup>(1)</sup> the disagreement between glass microelectrode and potentiometric dye  $V_m$  values suggested that microelectrode impalement probably compromised  $V_m$  measurements. Overall, digital imaging of N1E-115  $V_m$  was found to be sensitive, reproducible, fast, simple, and most important noninvasive. This technique has been successfully used in our laboratory for the measurement of chemically induced alterations in resting membrane potential in cultured N1E-115 cells.<sup>(15)</sup>

## ACKNOWLEDGMENTS

This research was supported through a University of Georgia Faculty Research Grant to W.S.K. and State and Hatch funds appropriated to the University of Georgia, College of Agricultural & Environmental Sciences Experiment Stations. Mention of brand names is for information only and does not imply endorsement.

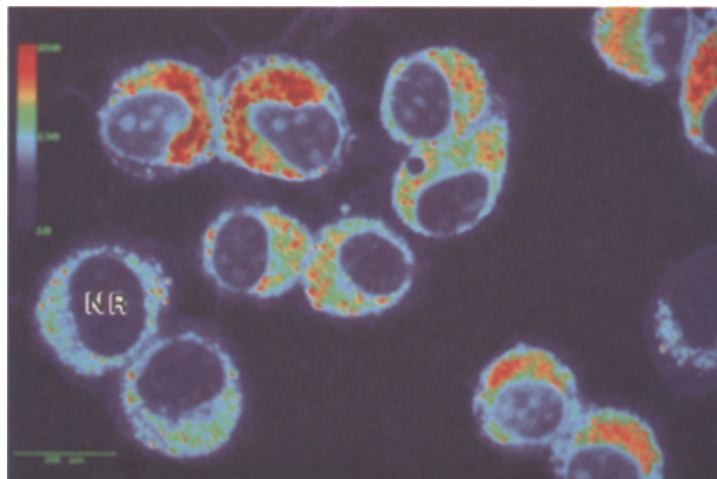


**Fig. 2.** TMRM-loaded N1E-115 cells. Nuclear region (NR) exhibited lower and more uniform fluorescence and therefore were convenient for quantifying organelle-free cytoplasmic fluorescence.

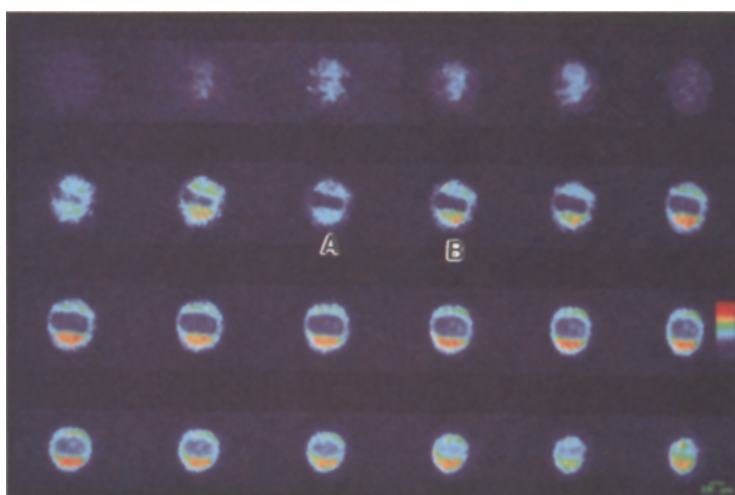


**Fig. 3.** Image montage of a series of optical sections obtained at 1- $\mu\text{m}$  intervals in N1E-115 cells loaded with 0.5  $\mu\text{M}$  TMRM. Sections A and B were the optimal images for scoring the average intracellular fluorescence intensity.

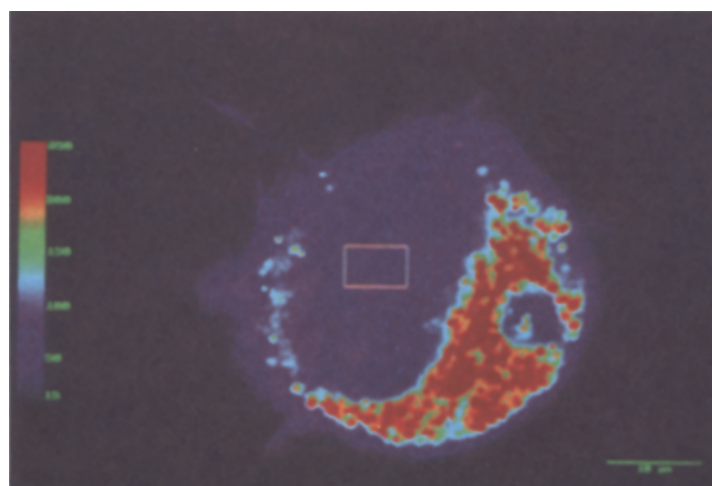


**Fig. 4A.** N1E-115 cell fluorescence image with the area of interest (AOI) placed in the nuclear region (A) and externally, in a region devoid of glowing debris (B). The cell was loaded with 0.5  $\mu\text{M}$  TMRM.

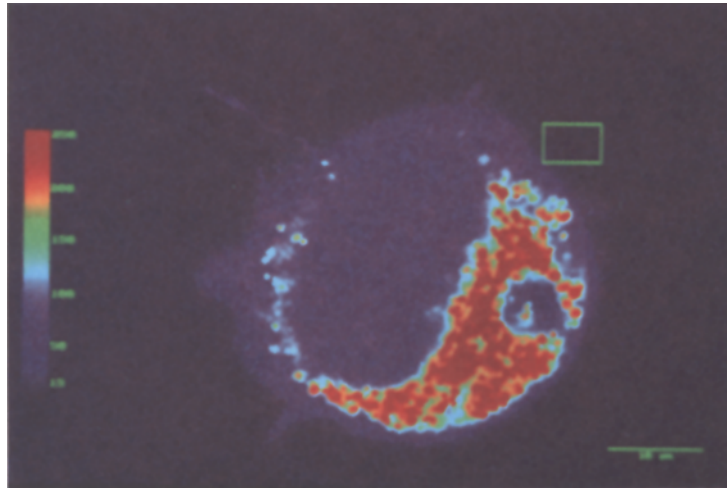


**Fig. 4B.** N1E-115 cell fluorescence image with the area of interest (AOI) placed in the nuclear region (A) and externally, in a region devoid of glowing debris (B). The cell was loaded with  $0.5 \mu\text{M}$  TMRM.

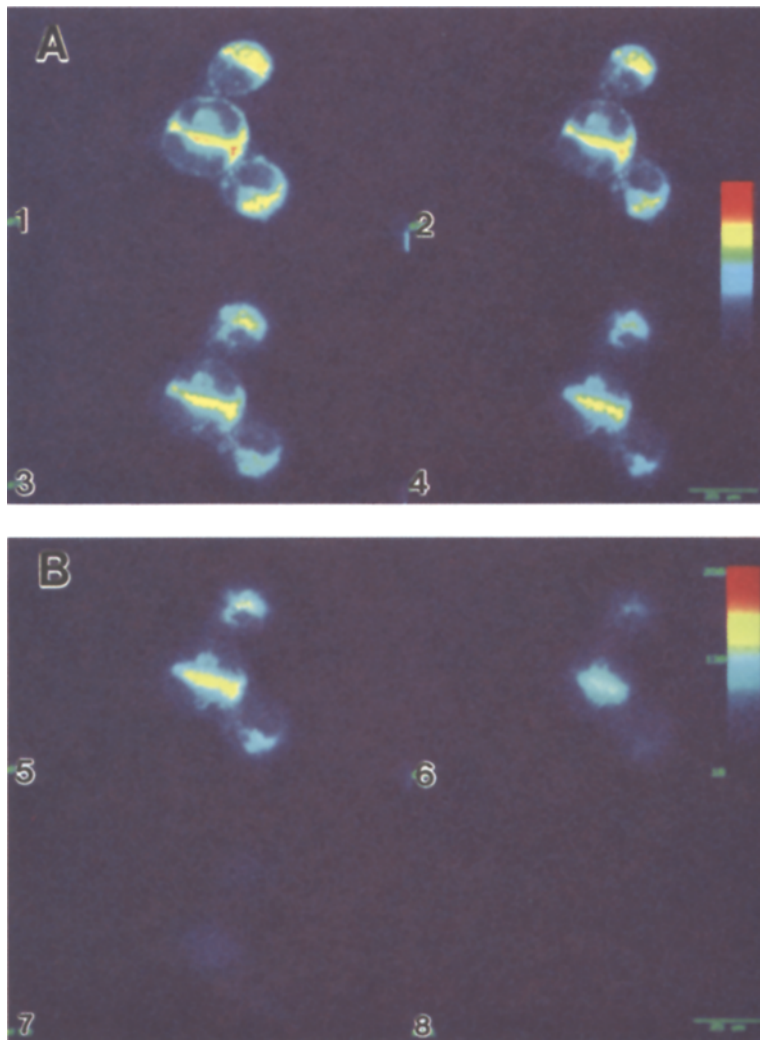


**Fig. 5.** Effect of valinomycin ( $0.1 \mu\text{M}$ ) on the fluorescence of TMRM-loaded N1E-115 cells at  $18^\circ\text{C}$ . Upon the addition of valinomycin, afflux of TMRM from cells to the medium occurred as illustrated by the fluorescence decrease in A (frames 1 and 2) to the background in B (frames 7 and 8).

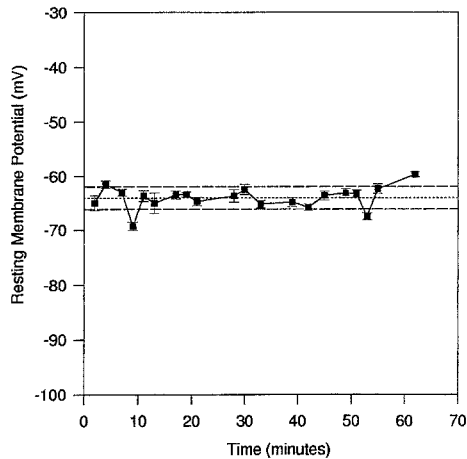


**Fig. 6.** Sequence of resting membrane potential measurements from single N1E-115 cells loaded with  $0.5 \mu\text{M}$  TMRM. Error bars are  $5 \times$  SE. Dotted lines represent overall average and 95% confidence interval.

## REFERENCES

1. W. S. Kisaalita and J. M. Bowen (1996) *Cyrotechnology* (in press).
2. J. Peacock, J. Minna, P. Nelson, and M. Nirenberg (1972) *Exp. Cell Res.* **73**, 367–377.
3. I. Spector, C. Palfrey, and U. Z. Littenauer (1975) *Nature* **254**, 121–124.
4. I. Spector (1981) in P. G. Nelson and M. Lieberman (Eds.), *Excitable Cells in Tissue Culture*, Plenum Press, New York, pp. 247–274.
5. Y. Kidokore (1981) in P. G. Nelson and M. Lieberman (Eds.), *Excitable Cells in Tissue Culture*, Plenum Press, New York, pp. 319–336.
6. B. Ehrenberg, V. Montana, M.-D. Wei, J. P. Wuskell, and L. M. Loew (1988) *Biophys. J.* **53**, 785–794.
7. L. M. Loew (1988) *Spectroscopic Membrane Probes*, CRC Press, Boca Raton, FL.
8. L. M. Loew (1993) in B. Matsumoto (Ed.), *Methods in Cell Biology: Cell Biological Applications of Confocal Microscopy*, Academic Press, New York, pp. 195–209.
9. R. K. Emaus, R. Grunwald, and J. J. Lemasters (1986) *Biochim. Biophys. Acta* **850**, 436–448.
10. Y. Kimhi, C. Palfrey, I. Spector, Y. Barak, and U. Z. Littauer (1976) *Proc. Natl. Acad. Sci. U.S.A.* **73**, 462–466.
11. H. C. Berg and S. M. Block (1984) *J. Gen. Microbiol.* **130**, 2915–2920.
12. A. Chalazonitis and L. A. Green (1974) *Brain Res.* **72**, 340–345.
13. K. S. Santone, G. S. Oakes, S. R. Taylor, and G. Powis (1986) *Cancer Res.* **46**, 2659–2664.
14. C. Cosgrove and P. Cobbett (1991) *Brain Res. Bull.* **27**, 53–58.
15. A. Hernandez and W. S. Kisaalita (1996) *Toxic. In Vitro* (in press).